Pharmacokinetics and computational profiling of *Spinifex littoreus*: Derived bioactive compounds against the Omicron XBB.1 variant

JOHN VEDHAMANI[1*], ISSAC NEWTON PAUL AJITHKUMAR[1], JAY SHREE MATHIVANAN[2*], SELVARAJ KARTHICK RAJA NAMASIVAYAM[3], CHANDRAMOHAN SUGANYA VASAVI[4] and SUVAIYARASAN SUVAITHENAMUDHAN[5,6]

[1]Department of Botany, Bishop Heber College (Autonomous), Affiliated to Bharathidasan University, Tiruchirappalli, Tamil Nadu 620017, India; [2]Department of Bioinformatics, Bishop Heber College (Autonomous), Tiruchirappalli, Tamil Nadu 620017, India; [3]Centre for Applied Research, Saveetha School of Engineering, Saveetha Institute of Medical and Technical Sciences (SIMATS), Saveetha University, Chennai, Tamil Nadu 602105, India; [4]Department of Artificial Intelligence, Amrita School of Artificial Intelligence, Bengaluru, Karnataka 560035, India; [5]Department of Research, Meenakshi Academy of Higher Education and Research (MAHER), Deemed to be University, Chennai, Tamil Nadu 600078, India; [6]Central Research Laboratory, Meenakshi Medical College Hospital and Research Institute (MMCHRI) Kanchipuram, Tamil Nadu 631552, India

Received April 7, 2025; Accepted August 21, 2025

DOI: 10.3892/wasj.2025.390

Abstract. The COVID-19 pandemic has presented a significant global public health crisis, putting forth a pressing need for natural remedies against the virus. The present study aimed to identify potential inhibitors of viral replication from *Spinifex littoreus* (Burm.f.) Merr. and to assess its ability to delay the binding of human angiotensin-converting enzyme 2 receptors with viral proteins through molecular docking. The screening of phytoconstituents from *Spinifex littoreus*, a coastal grass, was conducted and validated by gas chromatography-mass spectrometry (GC-MS) to discover potential severe acute respiratory syndrome coronavirus 2 (SARS-CoV-2) antagonists. A total of six different solvents were used for plant extraction via a Soxhlet apparatus followed by the qualitative estimation of secondary metabolites and quantification of major metabolites. The lead compound was then docked against the spike (S) glycoprotein of SARS-CoV-2 using the Autodock tool. GC-MS analysis revealed the presence of various secondary metabolites, with phenols being the most abundant. A compound named 1-methylene-2b-hydroxymethyl-3,3-dim ethyl-4b-(3-methylbut-2-enyl)-cyclohexane (SL-MHDC), eluted by both methanol and chloroform was identified as particularly abundant. Subsequently, the molecular docking of this compound against the spike (S) glycoprotein of SARS-CoV-2 had a binding energy of -4.86 kcal/mol, suggesting its potential as a therapeutic agent. On the whole, the present study demonstrates that *Spinifex littoreus* extracts contain beneficial compounds, particularly phenols that are effective against SARS-CoV-2. Further research is warranted for the validation of these findings in an experimental setup and the possible translation of this therapeutic intervention from bench to bedside.

Correspondence to: Dr Suvaiyarasan Suvaithenamudhan, Department of Research, Meenakshi Academy of Higher Education and Research (MAHER), Deemed to be University, Chennai, Tamil Nadu 600078, India
E-mail: bioinfosst@gmail.com

Dr Issac Newton Paul Ajithkumar, Department of Botany, Bishop Heber College (Autonomous), Affiliated to Bharathidasan University, Vayalur Main Road, Tiruchirappalli, Tamil Nadu 620017, India
E-mail: ipajith@gmail.com

*Contributed equally

Key words: *Spinifex littoreus*, gas chromatography-mass spectrometry, molecular docking, 1-methylene-2b-hydroxymethyl-3,3-dimethyl-4b-(3-methylbut-2-enyl)-cyclohexane, spike (S) glycoprotein, severe acute respiratory syndrome coronavirus 2

Introduction

The world has faced an unexpected public health crisis since 2019 due to the severe acute respiratory syndrome coronavirus type 2 (SARS-CoV-2) pandemic, known as COVID-19. The COVID-19 epidemic has caused an astounding number of fatalities and poses a distinct threat to the global food and public health systems. The devastating economic and social effects of the epidemic raise the prospect that many individualscould be pushed into extreme poverty (1-4). According to the World Health Organization (WHO) (https://covid19.who.int) (5), symptoms of COVID-19 can range from fever and

coughing to respiratory illness, bronchitis, renal disease, and, in extreme cases, death (6,7). WHO has documented 659,108,952 confirmed COVID-19 cases, including 6,684,756 fatalities. Up to December 21, 2022, 13,073,712,554 doses of vaccine had been administered (https://covid19.who.int) (5).

Understanding the life cycle of SARS-CoV-2 and its interactions with host cells is crucial for developing effective strategies to fight the virus. The ~30-kb genome of SARS-CoV-2 shares significant similarities with other coronaviruses, such as SAR-CoV and MERS-CoV, and contains two open reading frames (ORF)s1a and ORF1b, capable of translating numerous structural and non-structural proteins. The viral genome enters host cell membranes with the aid of the spike protein, facilitating attachment and membrane fusion via subunits S1 and S2. The rough endoplasmic reticulum synthesizes the 1,273-amino acid polyprotein precursor for the SARS-CoV-2 S glycoprotein, which is subsequently processed into two subunits, S1 and S2. These subunits play key roles in viral attachment to host cells and membrane fusion (8,9).

The predominant type I transmembrane S glycoprotein of the SARS-CoV-2 envelope incorporates with the cognate receptor of the host cell through membrane fusion. The S-surface glycoprotein specifies its target for host immune responses and serves as a prime target for antibody neutralization. Moreover, S-glycoprotein can promote the fusion of infected and uninfected cells to produce multinucleated giant cells by entering the plasma membrane through the secretory route (10,11). This could enable direct virus transmission across cells and possibly change the pathogen city of SARS-CoV-2. Spike proteins function as antiviral medications and vaccines due to their essential parts in viral infection and their ability to induce protective innate immune and cell-mediated adaptive immunity in susceptible hosts (12).

The four non-structural proteins identified in the virus are RNA polymerase, helicase, papain-like (PLpro) and 3-chymotrypsin-like (3Clpro) proteases (13). The viral replication and transcription are performed by proteases, Plpro and 3Clpro. Among these, the 3Clpro plays a critical role in the ability of the virusto reproduce (14). The key protease, also known as Mpro, is 3Clpro, and it is crucial for viral replication. One of the main targets for developing anti-SARS-CoVdrugs is the protease 3Clpro, which generates 11 of the 16 non-structural proteins (NSPs) that are produced when Plpro and 3Clpro cleave the PP chain into NSPs (15,16). According to apreviousstudy, the primary protease Mpro of COVID-19 shares 96% of its sequence with SARS-CoV (17). Despite being in development, effective therapeutic and preventive methods, such as medications and vaccines, are still lacking. Herein, it is necessary to identify novel therapeutic candidates that specifically target certain SARS-CoV-2 proteins to treat COVID-19. A computational method for identifying possible therapeutic candidates counter to the treatment of emerging infectious diseases such as COVID-19 is to create drugs based on protein structures (18,19).

The majority of anti-infective drugs are derived from secondary metabolites found in nature, sourced from microbial, oceanic, or plant origins (20,21). The pharmacological qualities of ~20% of all known plant species have been investigated; phytochemicalanalyseshave improved healthcare by aiding in the treatment of diseases such as cancer. Plants are able to generate a wide range of bioactive substances; fruits and vegetables, in particular, are able to store large amounts of phytochemicals that guard against harm from free radicals (22). The bioactive compounds have been classified as alkaloids, saponins, diterpenes and flavonoids. These bioactive compounds play a vital role in the discovery of new drugs from natural plants.

1-Methylene-2b-hydroxymethyl-3,3-dimethyl-4b-(3-methy lbut-2-enyl)-cyclohexane (SL-MHDC) is an important secondary metabolite and is isolated from *Spinifex littoreus* (*S. littoreus*) which belongs to the family Poaceae (23). This coastal grass thrives on dunes, characterized by extremely hard, in-rolled and curved leaves, with rough margins and spiky tips. The inflorescence of this plant is a raceme with an imbricate spikelet. This species forms substantial colonies and stabilizes dunes making it an effective sand binder (24). The ethnomedical history of *S. littoreus* indicates that the root extract of *S. littoreus* has been traditionally administered orally for the treatment of digestive disorders in the Purba Medinipur District of West Bengal, India (25). Root decoction is also used to treat joint and muscle pain (26). Furthermore, the therapeutic potential of this plant has been studied in order to elucidate its antimicrobial, antioxidant, anti-inflammatory and analgesic properties (27). This plant is also used traditionally as a diuretic medicine. The methanol and aquatic extract of this herb have been demonstrated in numerous pharmacological tests to have analgesic, anti-inflammatory and antibacterial effects (28). However, no therapeutic evidence is available for the antiviral property of the plant *S. littoreus,* as well as for the phytocompound MHDC. Dampalla *et al* (29) conducted a structure-guided design of conformationally constrained cyclohexane inhibitors of SARS-CoV-2 3CL protease. Considering this, the present study performed molecular docking analysis of the phytocompound MHDC identified from the plant *S. littoreus* against the 3CL main protease and spike glycoprotein of SARS-CoV-2 (30).

The present study aimed to investigate the phytochemical diversity of *S. littoreus* (Burm.f.) Merr. through preliminary phytochemical screening techniques and to validate the findings using gas chromatography-mass spectrometry (GC-MS) analysis. Furthermore, the present study sought to identify the inhibitory effects of the bioactive compound SL-MHDCon the key proteins of SARS-CoV-2, i.e., the spike protein. By leveraging the phytochemical diversity of this coastal grass, the authors aimed to contribute to the ongoing efforts to mitigate the devastating impact of COVID-19 on global health.

Materials and methods

Plant collection. S. littoreus was collected from Kunthukal Beach, Pamban, Tamil Nadu, India (latitude: 9.25323; longitude: 79.21829). The collected plants were authenticated, and the prepared herbarium sheets of the plantwas submitted to the Rapinat Herbarium and Centre for Molecular Systematics, St. Joseph's College, Tiruchirappalli, Tamil Nadu, India. (Voucher nos. J.V 001 and J.V 002).

Plant extraction. The young leaves of *S. littoreus* were separated from the plant, cleaned and shade-dried. The dried *S.*

littoreus leaves were mechanically pulverized. The powdered sample of *S. littoreus* was extracted with methanol and chloroform through the Soxhlet apparatus (Borosil Scientific Ltd.) for 16 h. To concentrate the collected extract, it was subjected to a rotary evaporatorand weighed. The extraction process was repeated until obtaining 5 g of powdered form of the extracts (31).

Preliminary phytochemical screening

Qualitative analysis. The qualitative analysis of carbohydrates, proteins, amino acids, tannins, saponins, flavonoids, alkaloids, terpenoids, steroids, phenols, glycosides, quinones, coumarins and anthraquinones was performed in six different solvent-mediated (aqueous, acetone, ethanol, methanol, chloroform and ethyl acetate) extracts of *S. littoreus*. All the chemicals and glassware used for the phytochemical screening were sourced from Royal Scientific Suppliers.

Carbohydrates. A total of two drops of Molisch reagent were added to 2 ml *S. littoreus* extract. Subsequently, 2 ml concentrated H_2SO_4 were added on the sides of the tube. The formation of purple colour was an indicator of the presence of carbohydrates (32).

Proteins. A few drops reagent were combined with 2 ml *S. littoreus* extract. The presence of proteinswas indicated by the production of a white precipitate, which subsequently turns brick red in colour (33).

Amino acids. In a boiling water bath, 1 ml *S. littoreus* extract along with 1 drop of ninhydrin solution was heated. The development of a purple colour indicated the presence of amino acids (32).

Tannins. In a test tube, 0.5 g powdered *S. littoreus* extract was heated in 20 ml distilled water, filtered and treated with 0.1% iron III chloride ($FeCl_3$). The samples were then observed for the development of brownish-green or blue-black coloration, indicating the presence of tannins (33).

Terpenoids. In a test tube, 5 ml *S. Littoreus*extract were used along with 2 ml $CHCl_3$. Subsequently, 3 ml concentrated H_2SO_4 were gently added to the mixture to form a layer. In the case that terpenoids are present, an interface with a reddish-brown colour will form (33).

Alkaloids (Mayer's test). A test tube was filled with 1 ml *S. littoreus* extract and 1 ml potassium mercuric iodide solution (Mayer's reagent). When this mixture was shaken gently, aprecipitate will be formed, confirming the presence of alkaloids (33).

Quinines. To 10 mg *S. littoreus* extract in isopropyl alcohol, one drop of concentrated sulfuric acid was added. The presence of quinones was indicated by the formation of a red colour (33).

Steroids. A total of 5 ml *S. littoreus* extract was mixed with 2 ml chloroform and concentrated H_2SO_4. A red colour appeared in the lower chloroform layer, indicating the presence of steroids (34).

Coumarin. A total of 2 ml *S. littoreus* extract was mixed with 3 ml 10% NaOH. The presence of coumarin was indicated by a yellow coloration (35).

Saponins. A total of 20 ml distilled water and 2 g powdered *S. littoreus* extract were heated together in a water bath and then filtered. Subsequently, 10 ml of the filtered sample were mixed with 5 ml distilled water in a test tube and vigorously shaken to form a stable, long-lasting froth. This was followed by the addition of three drops of extra virginolive oil to the froth to create an emulsion, indicating the presence of saponins (34).

Phenols. A few drops of $FeCl_3$ and 1 ml water were added to a test tube along with ~2 ml of the *S. littoreus* extract. The presence of a blue, green, red, or purple colour indicates the presence of phenols (35).

Anthraquinones (Borntrager's test). A total of 1 ml *S. littoreus* extract was added to a mixture of diluted ammonia, chloroform, or benzene. The presence of anthraquinone derivatives causes the ammonical layer to change colour from pink to bright red (35).

Flavonoids. *S. littoreus* extract was added to a test tube along with a few drops of a 1% NH_3 solution. Yellow colour concludes the presence of flavonoids (36).

Glycosides. *S. littoreus* extract was used along with 2 ml acetic acid and 2 ml chloroform. Once the mixture was cooledat room temperature, concentrated H_2SO_4 was added. The steroidal glycosides can be identified by their green colour appearance (37).

Quantitative screening of phytochemicals. The presence of alkaloids, terpenoids, phenolics, flavonoids and tannins was quantitatively estimated with their respective standard using the following methods:

Quantitative estimation of alkaloids. To estimate the quantity of alkaloids in *S. littoreus*, the extracts were treated with 5 ml bromocresol green and PBS. Atropine was used as a standard solution. Alkaloids were measured in milligrams of atropine equivalents per gram (mg AE/g) of chloroform extract of sample (38).

Quantification of terpenoids. A total of 500 g *S. littoreus* leaf powder was soaked in ice-cold 95% methanol and then centrifuged at 4,000 x g for 15 min at room temperature. The supernatant was mixed with 1.5 ml chloroform and 100 ml concentrated sulfuric acid. Following incubation at room temperature for 1.5-2 h in the dark, a brown precipitate appeared at the bottom, which was dissolved in 1.5 ml 95% methanol, and its absorbance was measured in the colorimeterat 538 nm (39).

Quantification of flavonoids. A colorimetric test was used to determine the quantity of flavonoids in the *S. littoreus* extract. To 1 ml of the extract, 0.3 ml of 10% aluminum chloride, 5% sodium nitrite and 2 ml of NaOH were added. The absorption spectrum of this mixture was measured using UV-visible instrumentat 510 nm. Similarly, a set of quercetin solutions was prepared and measured as standards. Flavonoid concentration was expressed as mg of quercetin equivalents per gram of extract (mg QE/g) (40).

Quantification of tannins. A total of 1 ml *S. littoreus* extract was mixed with 0.5 ml Folin-Ciocalteu reagent and 1 ml of 35% Na_2CO_3, followed by the addition of 7.5 ml distilled water. This mixture was then incubated at 30˚C for 30 min. Similarly, a set of tannic acid solutions was prepared, and the optical density was measured at 700 nm with an UV/visible spectrophotometer. The amount of tannins in the *S. littoreus* extract was expressed in milligrams of tannic acid equivalent per gram (mg TAE/g) (41).

Determination of total phenolics. A total of 1 ml *S. littoreus* extract was dispersed in 9 ml of distilled water along with 1 ml

of Folin-Ciocalteu and 10 ml of 7% Na_2CO_3 solution. This was incubated at 30˚C for 2 h at room temperature. Gallic acid was used as standard. Gallic acid equivalents (mg GAE/g) were used to represent mg of total phenolic component per gram of extract (42).

GC-MS analysis. The phytoconstituents present in the methanolic ethanol, ethyl acetate and chloroform extracts were screened using GC-MS analysis. The experimental condition of the instrument was a fused silica column filled with Elite-5MS (5% biphenyl, 95% dimethylpolysiloxane, 30 m, 0.25 mm ID, 250 m df) utilized in the analysis by the Clarus 680 GC, and the Helium carrier gas was used to separate the components at a constant flow rate of 1 ml/min. The injector temperature was set to 260˚C. The operating parameters of the mass detector were 240˚C for the transfer line, 240˚C for the ion source, 70 eV for the electron impact in the ionization mode, 0.2 sec for each scan, and 0.1 sec between scans. The component spectra were compared to a database of component spectrums maintained in the GC-MS NIST (2008) library (43,44). No standard compounds were used for the spectral comparison.

Drug suitability and pharmacokinetic profile. The physicochemical, pharmacokinetic and drug-likeliness properties of the compound SL-MHDC were predicted using the SwissADME server (http://www.swissadme.ch/) to optimize the compound based on its bioavailability, safety and efficacy (45,46).

Molecular docking

Ligand preparation. Based on the GC-MS results of *S. littoreus,* the chemical structure of the phytocompound SL-MHDCwas retrieved from the PubChem database (PubChem CID: 550196) as an optimized 3D ligand molecule. The downloaded ligand was prepared using the Autodock MGL application (https://autodock.scripps.edu/) by detecting its torsion root and saved in pdbqt format. This was then used for docking with AutodockVina (47,48).

Target protein preparation. The target protein selected for the study was the structure of SARS-CoV-2 XBB.1. The structure was downloaded from the protein data bank (PDB ID: 8IOV) in PDB format. The chain B spike glycoprotein (RBD) of XBB.1 was used as a target receptor for the docking analyses. The protein preparation was performed by removing the water molecules and the heteroatom within the structure. The structure was then examined for the missing residues and it was saved in pdbqt format. Both the optimized protein and ligand were then subjected to docking analysis using Autodock 4.2.6 software (49) to identify the affinity of the GC-MS-derived compound towards the SARS-CoV-2 XBB.1. The optimal pose with the least energy of binding was used for further analyses.

Molecular dynamics simulations (MDS). MDS is a computational paradigm that enables atomistic interrogation of biomolecular systems, which serves as a cornerstone in pharmaco-reconnaissance. Thus, MDS were executed using Desmond module (Schrödinger Suite) (50) (https://www.schrodinger.com/platform/products/desmond/). The SARS-CoV-2 XBB.1 spike glycoprotein complexed with SL-MHDC was solvated via system builder by employing TIP4P aqueous solvation within an orthorhombic solvent box. Moreover, the cell size was 49.6x68.1x51.7 Å, as well as the solvent buffer extending 10 Å, which is beyond the protein in all Cartesian directions. As a corollary, OPLS_2005 force field was deployed to parameterize molecular energetics. Judiciously, electrostatic neutrality was achieved by the incorporation of counter ions (Na^+ and Cl^-) that was followed by constrained energy minimization with the exorbitant of 2,500 iterations, as well as the convergence thresholds of 1 kcal/mol/Å. Furthermore, the present study exploited NPT ensemble with the Nose-Hoover thermostat algorithm which is lauded for thermal fluctuations set at a reference temperature of 300 K. A >30 nsec trajectory was generated and the post-simulation analyses encompassed with Root-mean-square deviation (RMSD) and the interrogation of SARS-CoV-2 XBB.1 integrated with SL-MHDC complex persistent was designated against the binding locus.

Results

Screening of phytoconstituents. The preliminary phytochemical screening of *S. littoreus* was carried out to identify the presence of secondary metabolites, such as alkaloids, flavonoids, tannins, saponins, glycosides, quinones, coumarins, steroids, phenols, terpenoids and anthraquinones using six different solvents (aqueous, acetone, ethanol, methanol, chloroform and ethyl acetate). Among these, the chloroform extract revealed sevensecondary metabolites and one primary metabolitein *S. littoreus* followed by the acetone, methanol and ethanol extracts, which revealed sixsecondary metabolites and one primary metabolite. The ethyl acetate extract only revealed four compounds (Table I).

The total amount of terpenoids, phenols, tannins, alkaloids and flavonoids present in the *S. littoreus* extract was estimated using quantitative analysis with their respective standards. The findings indicated the presence of all five examined compounds in the *S. littoreus* plant, albeit in varying concentrations: Phenol (7.5 mg/g), terpenoids (5.05 mg/g), flavonoids (0.4 mg/g), tannin (0.2 mg/g) and alkaloids (0.19 mg/g). The concentrations of phenol, terpenoids, flavonoids, tannin and alkaloids in the *S. Littoreus* leaflet extract are illustrated in Fig. 1. Among these compounds, phenol and terpenoids accumulated at higher levels in the *S. Littoreus* leaflet. Additionally, the leaflet extract of *S. Littoreus* also contained trace levels of alkaloids, tannins and flavonoids.

Following the preliminary screening, GC-MS analysis of the ethanol, methanol, chloroform and ethyl acetate extracts of *S. Littoreus* leaves was performed; this revealed the presence of various active phytocompounds. A total of 33 different compounds were eluted from this plant. Among these 33 compounds, 1-methylene-2β-hydroxymethyl-3,3-dimethyl-4β-(3-methylbut-2-enyl)-cyclohexane (28.834%), hexadecane (19.962%), tetratetracontane (18.416%), octacosane (16.136%), octadecanal (15.833%), heptacosane (14.574%), 2-methyl-3-(3-methyl-but-2-enyl)-2-(4-methyl-pent-3-enyl)-oxetane (14.434%) had the high percentage area. The names, molecular formulas and area percentages of the screened phytoconstituents are presented in Table II, and the biological activities with the 2D structures of the compounds are presented in Table SI. The chromatogram images of the tested samples are illustrated in Figs. 2-5.

Table I. Qualitative assessment of phytochemicals.

Metabolites	Solvents					
	Aqueous	Acetone	Ethanol	Methanol	Chloroform	Ethyl acetate
Primary metabolites						
Carbohydrates	+	-	+	+	+	-
Proteins	-	-	-	-	-	-
Amino acids	-	-	-	-	-	-
Secondary metabolites						
Alkaloids	-	-	+	+	+	-
Flavonoids	-	+	+	+	+	+
Tannins	+	+	-	+	-	-
Saponins	+	-	+	-	+	-
Glycosides	+	+	-	-	-	-
Quinones	-	+	+	+	+	+
Coumarins	+	+	+	+	+	+
Steroids	-	-	+	+	+	+
Phenols	+	+	-	-	-	-
Terpenoids	-	-	-	-	+	-
Anthraquinones	-	-	-	-	-	-

+, present; -, absent.

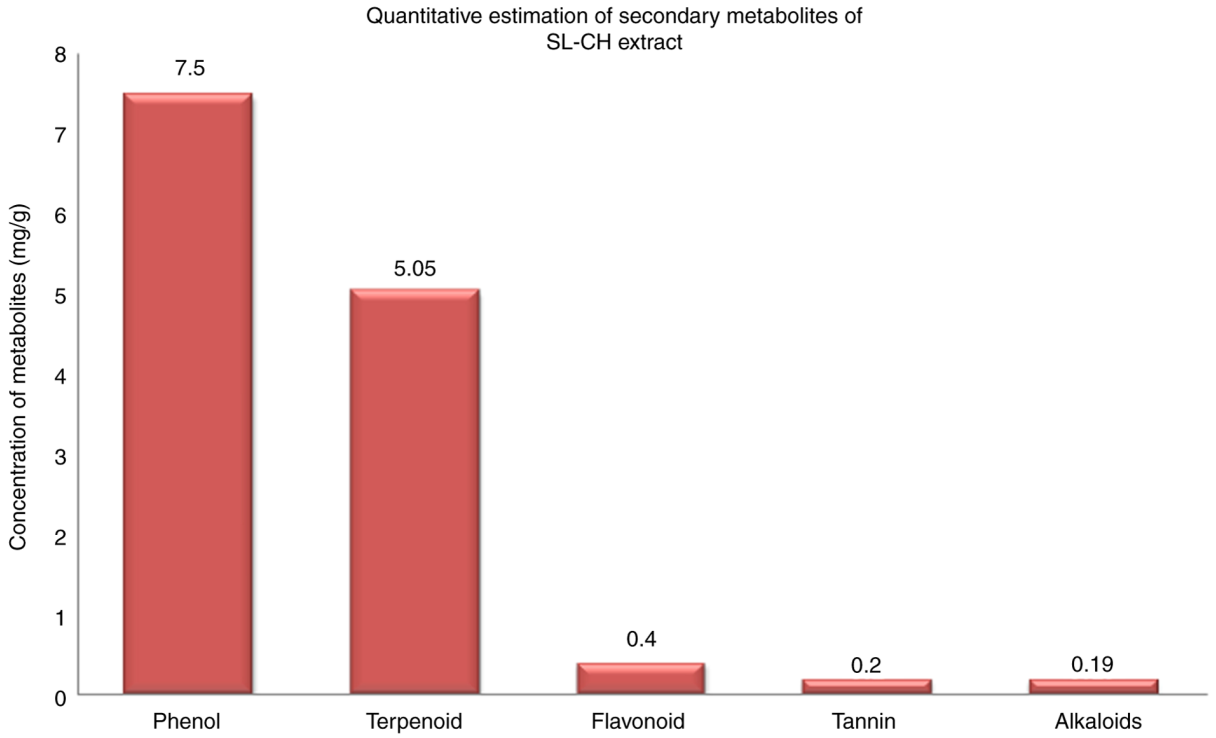

Figure 1. Concentration of phenol, terpenoids, flavonoids, tannin and alkaloids in *Spinifex littoreus* leaflet.

Assessment of drug-likeliness and pharmacokinetic profiles. The compound selected from the GC-MS analysis was subjected to *in silico* drug-likeliness and pharmacokinetic prediction to investigate its absorption, distribution, metabolism and toxicity profiles, and to evaluate whether there are any violations in Lipinski's rule of 5. According to Lipinski's rule of 5, the molecular weight should be <500 g/mol, not >10 g/mol, with >5 hydrogen bond acceptors and donors, and a log P-value >5. It is important to consider any bioactive compounds as a lead molecule in

Table II. Phytoconstituents present in the extract of *Spinifex littoreus* (Burm.f.) *Merr*.

Chloroform				Methanol				Ethanol				Ethyl acetate			
Name of the compound	Molecular formula	RT	Area %	Name of the compound	Molecular formula	RT	Area %	Name of the compound	Molecular formula	RT	Area %	Name of the compound	Molecular formula	RT	Area %
Phenol, 2,4-bis (1,1-dimethyl)	$C_{14}H_{22}O$	14.618	2.537	1,2-benzenedicarboxylic acid, butyl octyl ester	$C_{20}H_{30}O_4$	19.885	2.118	Methanediamine, n,n,n',n'-tetraethyl	$C_9H_{22}N_2$	19.275	1.090	3-tetradecane, (z)	$C_{14}H_{28}$	15.689	1.921
3-tetradecene, (Z)	$C^{14}H_{28}$	15.699	2.498	Alpha-bisabolol	$C_{15}H_{26}O$	24.287	1.229	N-hexadecanoic acid	$C_{16}H_{32}O$	19.896	0.918	1,6;3,4-dianhydro-2-deoxybeta-d-lyxo-hexopyranose	$C_6H_8O_3$	17.324	1.094
3-octadecene, (E)	$C_{18}H_{36}$	18.095	3.790	Hexatriacontane	$C_{36}H_{74}$	24.813	2.076	1-iodo-2-methylundecane	$C_{12}H_{25}I$	23.987	0.683	3-tetradecane, (z)	$C_{14}H_{28}$	18.085	3.427
N-Hexadecanoic acid	$C_{16}H_{32}O_2$	19.911	0.939	1-iodo-2-methylundecane	$C_{12}H_{25}I$	25.618	2.854	Hexadecane	$C_{16}H_{34}$	24.818	2.361	N-hexadecanoic acid	$C_{16}H_{32}O$	19.891	1.593
N-tetracosanol	$C_{24}H_{50}O$	20.246	3.852	1-methylene-2b-hydroxymethyl-3,3-dimethyl-4b-(3-methylbut-2-enyl)-cyclohexane	$C_{15}H_{26}O$	25.728	28.834	Hexadecane	$C_{16}H_{34}$	25.623	5.859	N-tetracosanol-1	$C_{24}H_{50}O$	20.236	2.714
1-hexacosanol	$C_{26}H_{54}O$	22.187	3.300	1-iodo-2-methylundecane	$C_{12}H_{25}I$	26.388	3.628	Sulfurus acid, butyl decyl ester	$C_{14}H_{30}O_3S$	26.398	10.570	Oleic acid	$C_{18}H_{34}O_2$	21.661	1.135
1-hexacosanol	$C_{26}H_{54}O$	23.947	1.541	2-methyl-3-(3-methyl-but-2-enyl)-2-(4-methyl-pent-3-enyl)-oxetane	$C_{15}H_{26}O$	26.503	14.434	Hexadecane	$C_{16}H_{34}$	27.189	13.820	1-docosene	$C_{22}H_{44}$	22.171	1.852
1-octonal,2-butyl	$C_{12}H_{26}O$	23.987	0.807	5-ethyl-1-nonane	$C_{11}H_{22}$	26.768	1.199	Hexadecane	$C_{16}H_{34}$	28.064	19.962	1-iodo-2-methylundecane	$C_{12}H_{25}I$	24.813	2.223
Hexadecane	$C_{16}H_{34}$	24.818	2.139	1-iodo-2-methylundecane	$C_{12}H_{25}I$	27.173	3.313	Octacosane	$C_{28}H_{58}$	29.054	14.993	Nonadecane	$C_{19}H_{40}$	25.613	5.161
DI-N-Octyl phthalate	$C_{24}H_{38}O_4$	25.118	1.250	Octadecanal	$C_{18}H_{36}O$	27.539	15.833	Tetratetracontane	$C_{44}H_{90}$	30.220	18.416	Hexadecane	$C_{16}H_{34}$	26.393	7.837

Table II. Continued.

Chloroform				Methanol				Ethanol				Ethyl acetate			
Name of the compound	Molecular formula	RT	Area %	Name of the compound	Molecular formula	RT	Area %	Name of the compound	Molecular formula	RT	Area %	Name of the compound	Molecular formula	RT	Area %
Nonadecane	$C_{19}H_{40}$	25.623	3.660	Hexatriacontane	$C_{36}H_{74}$	28.049	4.191	Nonadecane	$C_{19}H_{40}$	31.575	8.984	Hexadecane	$C_{16}H_{34}$	27.173	11.655
1-Methylene-2b-hydroxymethyl-3,3-dimethyl-4b-(3-methylbut-2-enyl)-cyclohexane	$C_{15}H_{26}O$	25.838	12.558	Octadecylpentafluoropropionate	$C_{21}H_{37}F_5O$	29.039	2.659	Octadecanol	$C_{18}H_{36}O$	32.316	2.345	Heptacosane	$C_{27}H_{56}$	28.049	14.574
Nonadecane	$C_{19}H_{40}$	26.403	7.461	1-hexacosanol	$C_{26}H_{54}O$	29.169	11.664					Tetratetracontane	$C_{44}H_{90}$	29.039	11.422
2-methyl-3-(3-methyl-but-2-enyl)-2-(4-methyl-pent-3-enyl)-oxetane	$C_{15}H_{26}O$	26.513	9.114	Hexadecanal	$C_{16}H_{32}O$	29.594	2.114					Octacosane	$C_{28}H_{58}$	30.200	16.136
Hexadecane	$C_{16}H_{34}$	27.184	9.437	1-decanol, 2-ethyl	$C_{12}H_{26}O$	30.195	2.677	-	-	-	-	Cis-9,10-epoxyoctadecane-1-ol	$C_{18}H_{36}O_2$	30.425	1.004
Hexadecane	$C_{16}H_{34}$	28.064	11.368	Undecanal	$C_{11}H_{22}O$	31.545	1.176	-		-	-	Hexatriacontane	$C_{36}H_{74}$	31.555	6.475
Tetracontane, 3,5, 24-trimethyl	$C_{43}H_{88}$	29.059	9.041	-	-	-		-	-	-	-	Pentadecanal	$C_{15}H_{30}O$	32.306	9.777
Nonadecane	$C_{19}H_{40}$	30.210	8.803	-	-	-	-	-	-	-	-	-	-	-	-
1-octanol,2-butyl	$C_{12}H_{26}O$	31.571	-	-	-	-	-	-	-	-	-	-	-	-	-
Pentadecanal	$C_{15}H_{30}O$	32.316	-	-	-	-	-	-	-	-	-	-	-	-	-

Table III. Physicochemical properties of the compound selected through gas chromatography-mass spectrometry analysis.

Compound name	Molecular weight g/mol (<500)	H-bond acceptors (<10)	H-bond donors (<5)	MlogP (<4.15)	Lipinski violations
1-Methylene-2b-hydroxymethyl-3,3-dimethyl-4b-(3-methyl but-2-enyl)-cyclohexane	222.37	1	1	3.56	0

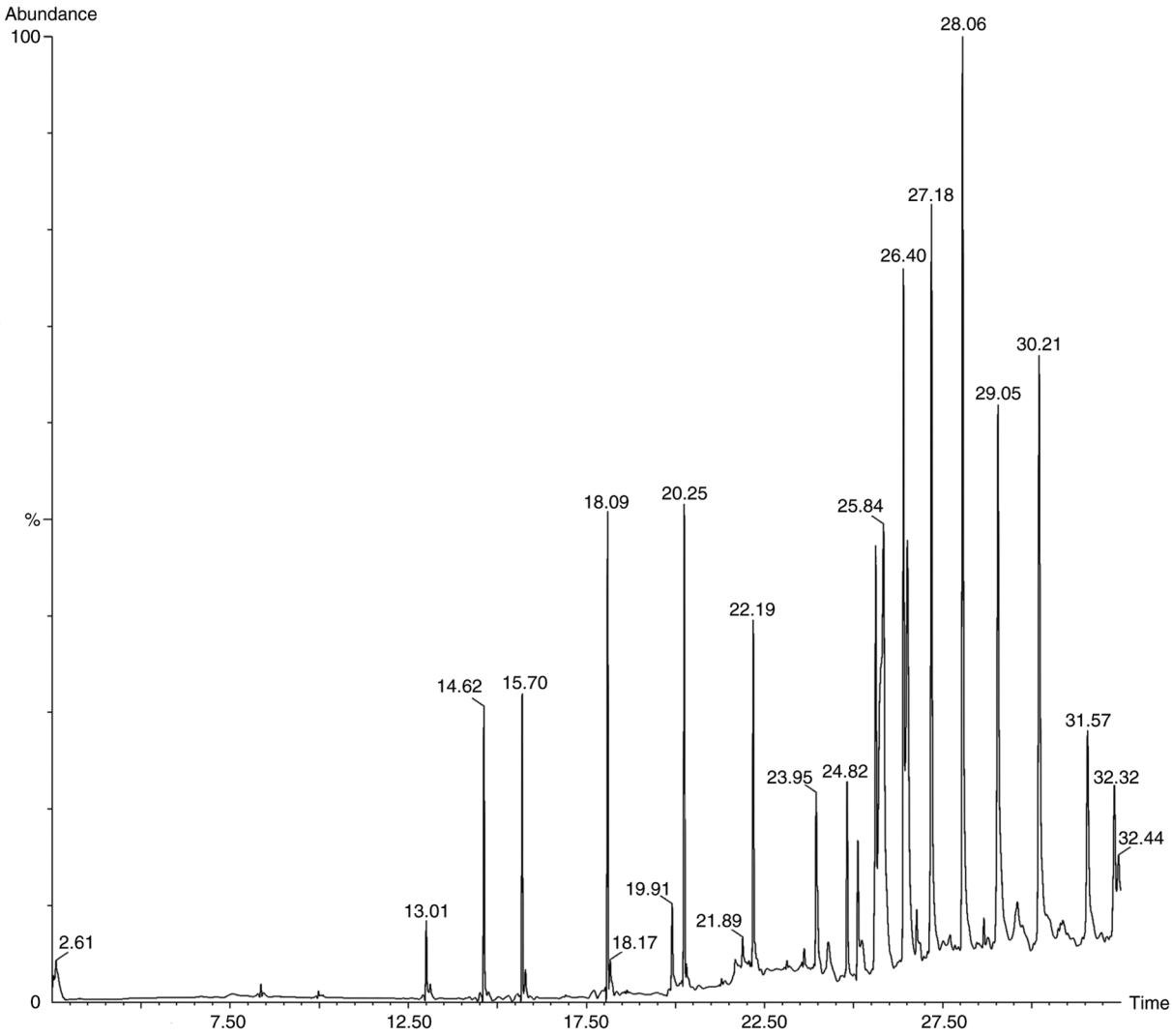

Figure 2. Gas chromatography-mass spectrometry chromatogram image of chloroform-mediated *Spinifex littoreus* extracts exhibiting 20 different peaks.

the process of drug discovery. From the results of ADME analysis, it was identified that there were 0 violations in Lipinski's' rule of 5, the molecular weight of the compound was observed to be 222.37 g/mol, there was 1 hydrogen bond donor and acceptor, the MLogP of the compound was 3.56 (Table III). Additionally, the pharmacokinetic properties of the compounds were evaluated, including the calculation of inhibition, which includes the subfamilies of cytochrome P450, such as CYP2C19, CYP2C9, CYP1A2, CYP2D6 and CYP3A4, and BBB permeant. All these results, including the drug likeliness of the compounds are presented in Tables IV and V. This suggests that the compound has drug-like properties, as it meets the Lipinski's and Ghose's rules, which evaluate the properties for drug-likeliness, indicating that it falls within the range of properties commonly found in known drugs. The compound meets Veber's criteria suggesting its good oral availability potential. In addition, the compound meets the Egan rule, indicating it is less likely to be a P-glycoprotein substrate.

Docking analyses results. To evaluate the activity of the compound SL-MHDC against the SARS-CoV-2 XBB.1

Table IV. Pharmacokinetic properties of the compound selected from chromatography-mass spectrometry analysis.

Compound name	Gi absorption	BbbPermeant	P-Gp substrate	Cyp1a2 inhibitor	Cyp2c19 inhibitor	Cyp2c9 inhibitor	Cyp2d6 inhibitor	Cyp3a4 inhibitor
1-Methylene-2b-hydroxymethyl-3,3-dimethyl-4b-(3-methylbut-2-enyl)-cyclohexane	High	Yes	No	No	No	Yes	No	No

Table V. Drug-likeness of the compound selected through chromatography-mass spectrometry analysis computed using SWISS-ADME.

Compound name	Lipinski	Ghose	Veber	Egan	Muegge	Bioavailability score
1-Methylene-2b-hydroxymethyl-3,3-dimethyl-4b-(3-methylbut-2-enyl)-cyclohexane	Yes; 0 violation	Yes	Yes	Yes	No, 1 violation: heteroatoms <2	0.55

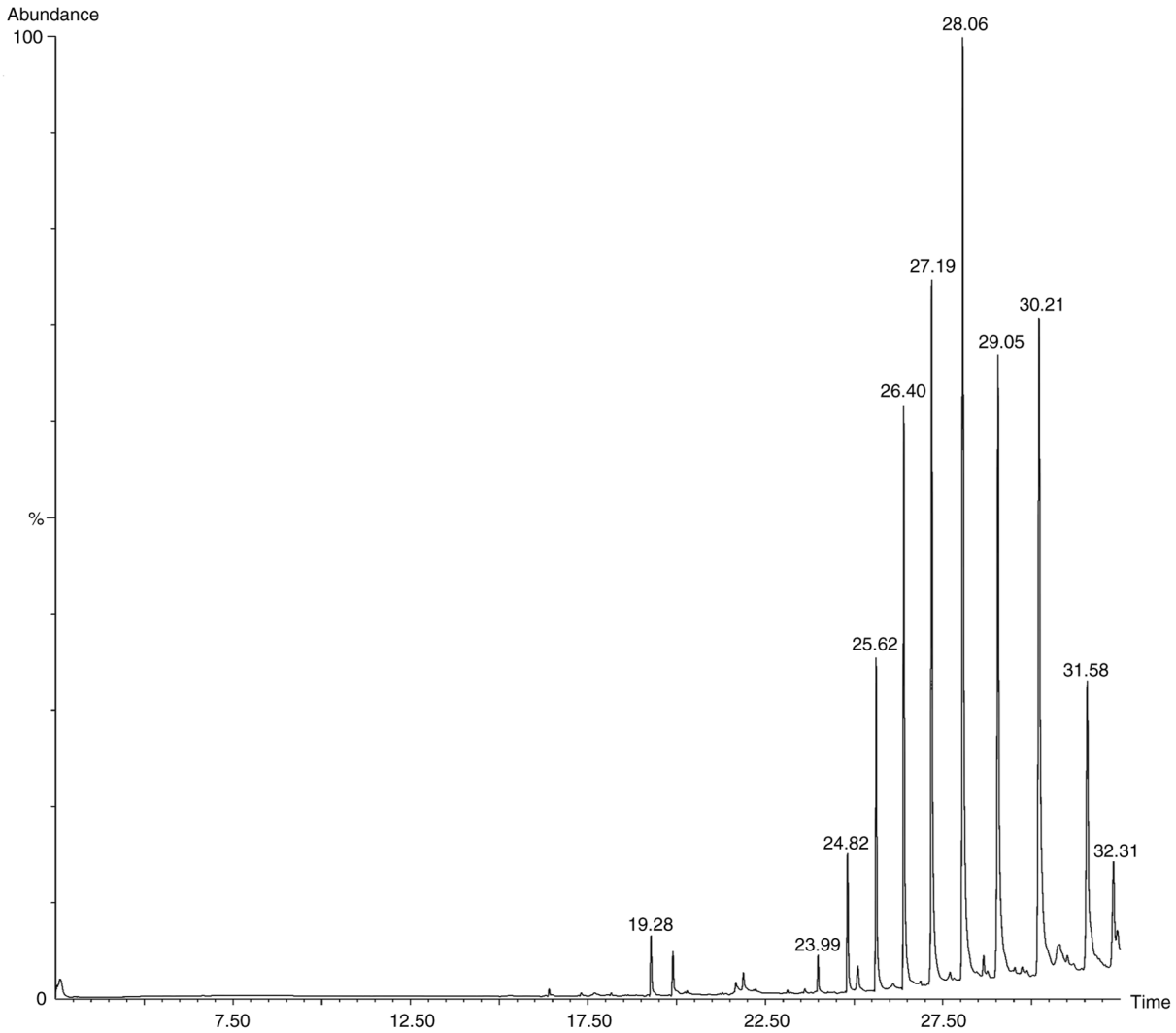

Figure 3. Gas chromatography-mass spectrometry chromatogram image of the ethanolic extract of *Spinifex littoreus* exhibiting 11 different screened compounds.

spike RBD (PDB ID: 8IOV), both the target protein and the selected ligand were subjected to docking analyses. The computational docking was performed using the AutoDock tool, which generated binding modes in the lowest energy

Table VI. Docking results of 1-methylene-2b-hydroxymethyl-3,3-dimethyl-4b-(3-methylbut-2-enyl)-cyclohexane with SARS-CoV-2 XBB.1.

Compound name	Protein ID	Binding energy (kcal/mol)	No. of H-bonds	H-Bond forming residues	Bond length (Å)
1-Methylene-2b-hydroxymethyl-3,3-dimethyl-4b-(3-methylbut-2-enyl)-cyclohexane	8IOV	-4.86	2	LYS444 ASN448	3.08 2.58

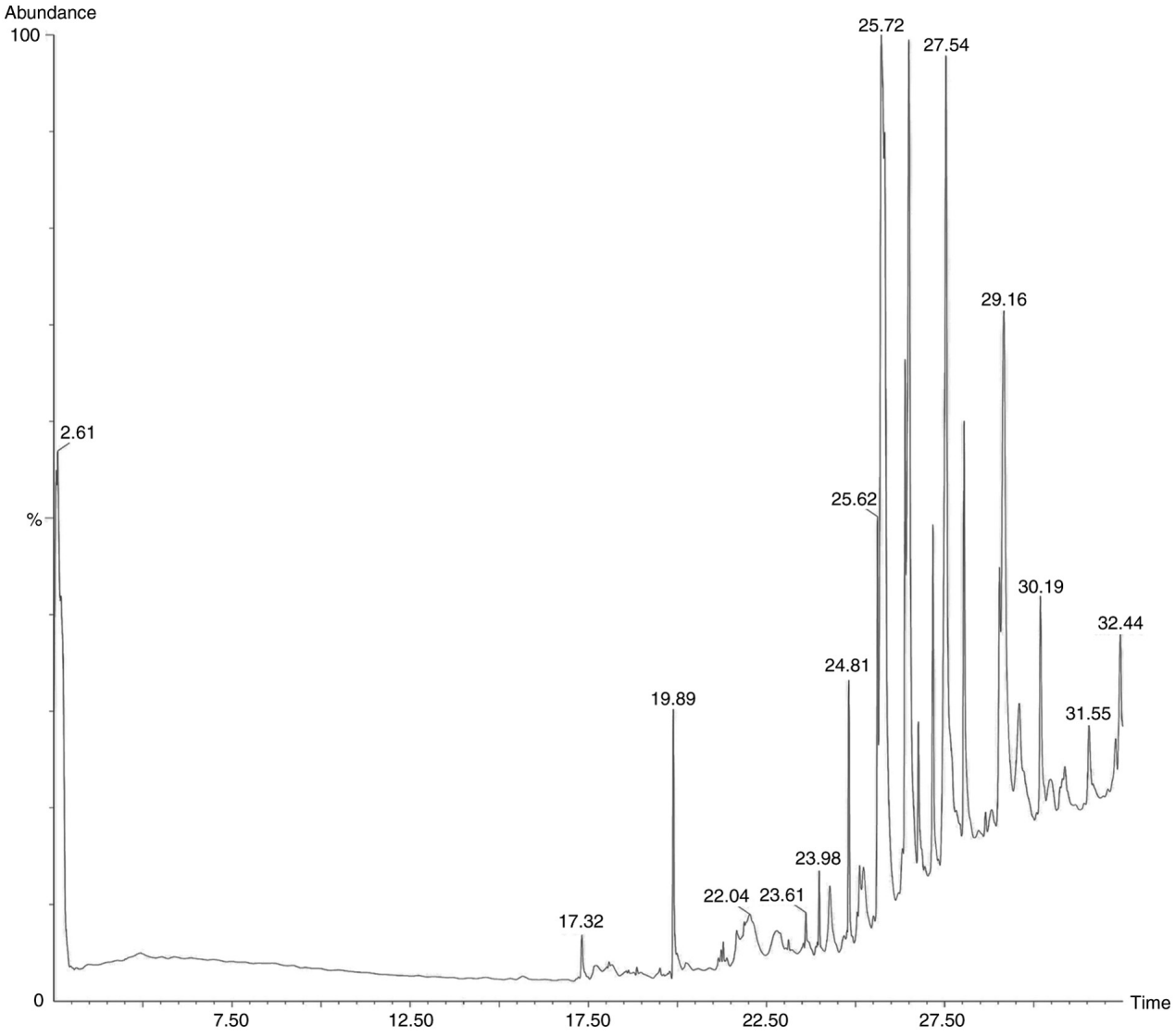

Figure 4. Gas chromatography-mass spectrometry chromatogram of methanolic extract of *Spinifex littoreus*.

state. The binding energy of SL-MHDC with the XBB.1 was observed to be -4.86 kcal/mol. This interaction formed two conventional hydrogen bonds with the amino acid residues LYS444 (B) and ASN 448 (B) (Fig. 6) in the spike glycoprotein. The bond lengths were measured as 3.08 and 2.58 Å, respectively (Table VI). The other non-bonded interactions include the Vander der Waals interaction formed by the residues, such as LEU 441 (B), ASP 442 (B), ARG 509 (B), THR 345 (B), PHE 347 (B), THR 346 (B), ASN 450 (B), the Pi-sigma and Pi-Alkyl interaction was formed by TYR 451 (B) (Fig. 7). Hence, from the molecular docking it could be inferred that the compound SL-MHDC *S. littoreus* can be used as a putative inhibitor potent drug against the spike glycoprotein of XBB.1.

Molecular dynamics evaluation of the XBB.1 - SL-MHDC complex. In order to assess conformational stability and interaction fidelity of the SARS-CoV-2 XBB.1 spike glycoprotein

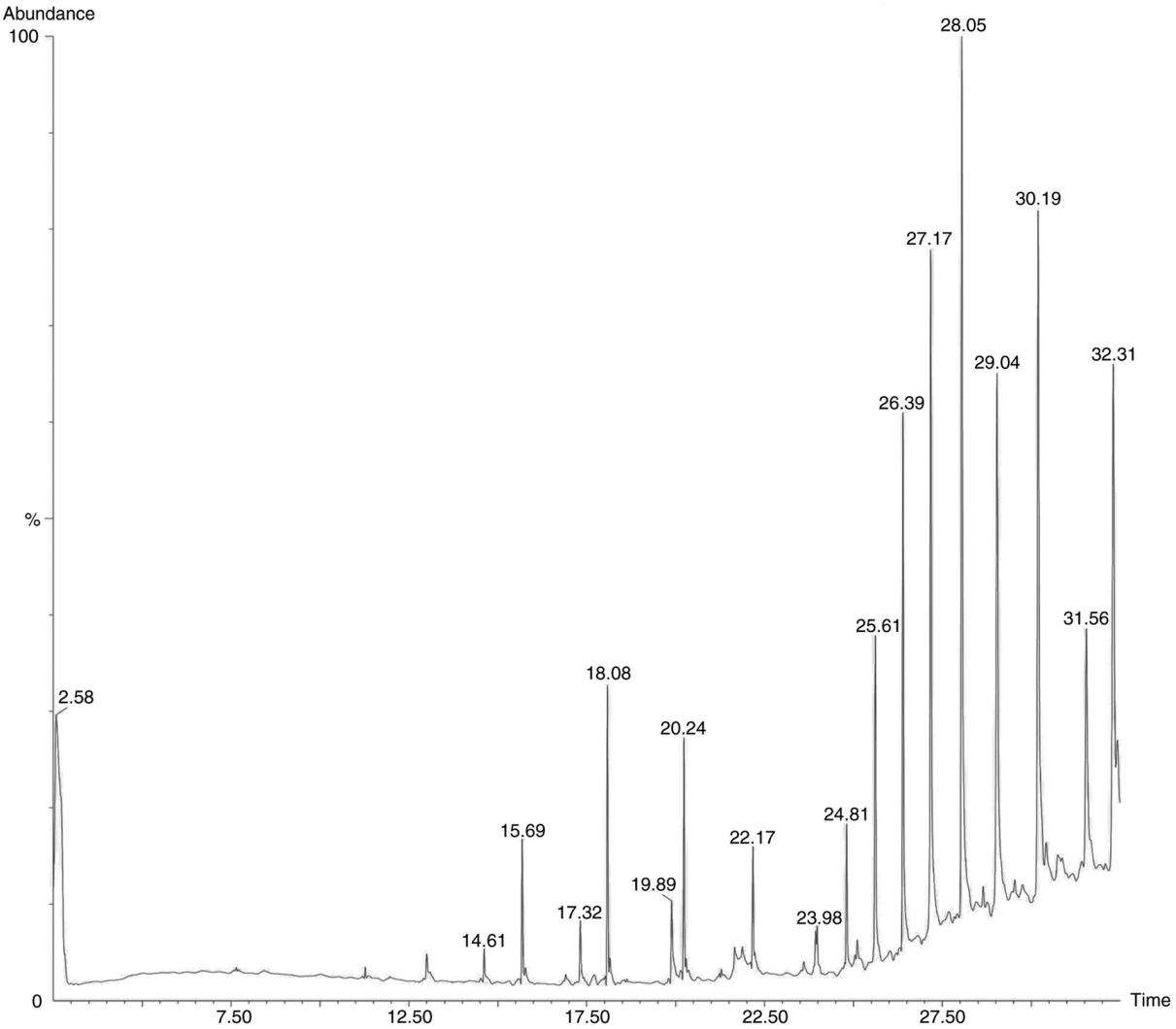

Figure 5. Gas chromatography-mass spectrometry chromatogram of *Spinifex littoreus* ethyl acetate extract exhibiting 17 peaks.

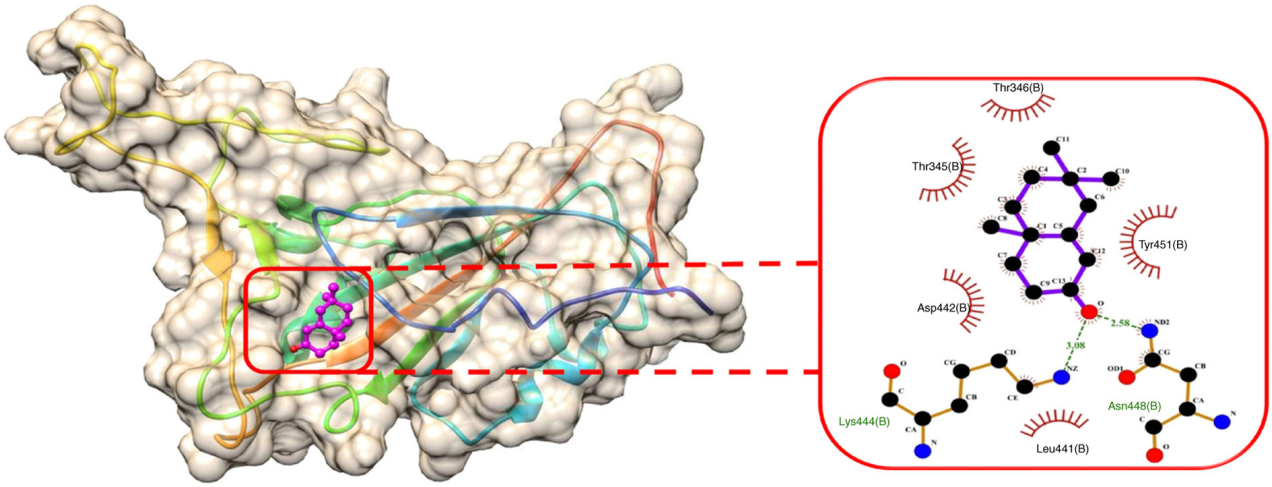

Figure 6. Spike glycoprotein and 1-methylene-2b-hydroxymethyl-3,3-dimethyl-4b-(3-methylbut-2-enyl)-cylohexane depicting the interaction and binding of the compound with spike glycoprotein.

complexed with the phyto-ligand SL-MHDC, explicit MDS were effectuated for a 30 nsec. The simulation encompassed with the canonical analyses including RMSD profiling and protein-ligand contact mapping (Fig. 8).

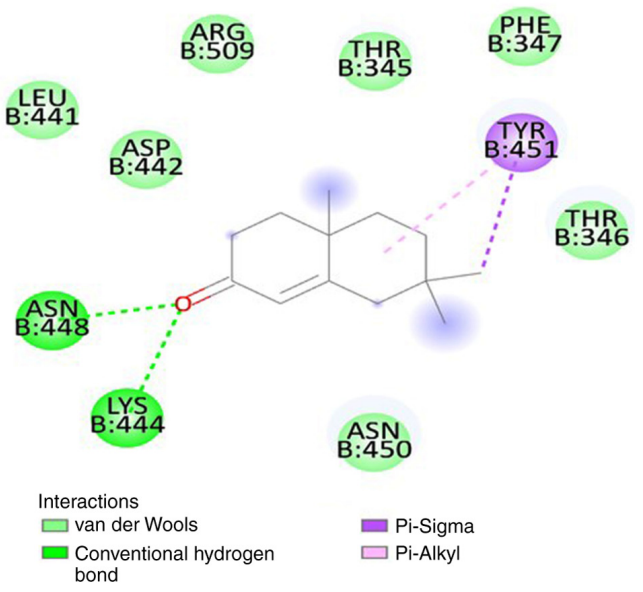

Figure 7. 2D diagram representing the interaction between the spike glycoprotein and1-methylene-2b-hydroxymethyl-3,3-dimethyl-4b-(3-methylbut-2-enyl)-cylohexane.

Discussion

Phytochemicals are non-nutritive plant compounds considered to be beneficial for human health due to their potential therapeutic properties (51). Worldwide, due to their perceived effectiveness, scientists are investigating the potential use of pharmacologically active compounds derived from therapeutic plants. Of note, 80% of individuals globally utilise herbal medications due to their effectiveness, affordability, non-narcotic nature and lack of adverse effects (52). The present study aimed to identify a potent anti-coronaviral compound from a coastal grass *S. Littoreus* by screening its phytoconstituents. The preliminary phytochemical screening of *S. Littoreus* leaflet revealed the presence of major constituents, such as alkaloids, flavonoids, tannins, saponins, glycosides, quinones, coumarins, steroids, phenols and terpenoids. Chandran *et al* (53) in 2014 also supported the presence of phytocompounds of alkaloids, flavonoids, saponins and phenol in *S. littoreus*. These compounds are considered therapeutically significant metabolites due to their pharmacological activities, such as anti-malarial, anticancer, anti-microbial, anti-ulcer, anti-inflammatory and diuretic actions (54-58). Quantitative analysis revealed the marked abundance of phenolic compounds and terpenoids. Phenolic compounds play a vital role in the plant by protecting them from UV radiations, pathogenic microorganisms and parasites (59). Additionally, they can serve as sources of anti-carcinogenic and anti-mutagenic agents (60). Terpenoids play a crucial role in plant defence against biotic and abiotic stresses and as signal molecules for pollination insects (61). Along with this, they are also effective in preventing and treating various diseases, including cancer. They do have pharmacological importance as antimicrobial, antifungal, antiparasitic, antiviral, anti-allergenic, antispasmodic, antihyperglycemic, anti-inflammatory and immunomodulatory agents (62). A trace amount of flavonoids, tannin and alkaloids was also recorded, which in plants serve as a defence system and possesses antimicrobial and anti-inflammatory properties (63). While quantitative determination is a key technique used to set the standard of a crude medication, solvent efficiency in phytochemical extraction provides an early indicator of medicinal grade (64).

One of the most effective methods for determining the components of volatile matter, including alcohols, esters, acids and long-chain hydrocarbons, is GC-MS. Considering the molecular formula, peak area and retention time, it was established that the phytochemical substances were what they claimed to be (65). The GC-MS results in the present study revealed the presence of pharmaceutically important phytoconstituents. GC-MS in conjunction with methanolic and aqueous extraction has been extensively utilized to discover phytochemicals of clinical significance (66,67). Tetradecanoic acid can be used as a lubricant, hypercholesterolemic, anticancer, antioxidant and cosmetic. Hexadecanoic acid functions as a pesticide, flavouring agent, 5-alpha-reductase inhibitor, lubricant, haemolytic, antifibrinolytic, nematicide and anti-alopecic. Octadecanoic acid, or stearic acid, is used in the cosmetics, flavour and perfumery industries (68). Heptacosane, heptadecane, octacosane and pentacosane have all been shown to have antioxidant activity (69-71). Undecanal and N-tetracosanol have potential antiviral properties (72). The compound 1-methylene-2b-hydroxymethyl-3,3-dimethyl -4b-(3-methylbut-2-enyl)-cyclohexane wasthe first hit in the methanolic and chloroform extract of *S. littoreus*.

As there were no violations in Lipinski's rule of 5, the compound was taken as a lead compound for further analysis. Additionally, the binding affinity between the selected target and the compound indicated the lowest energy binding of -4.86 kcal/mol, with two hydrogen bonds formed between residues LYS444 and ASN448, respectively. Furthermore, the stability of the complex was evaluated by the RMSD (Fig. 8A); it was inferred that complex became equilibrated around 13 nsec and it fluctuates around its average value. According to the protein-ligand contact analysis (Fig. 8B), residues interactions with the SL-MHDC were meticulously monitored throughout the simulation. Protein-ligand contacts are stratified into hydrogen bonding, hydrophobic interactions, ionic linkages and water-mediated bridges. A total of 35 residues were engaged with SL-MHDC among which His339, Asn343, Ala344, Thr345, Asn448, Asn450, Ala484, Arg498, and Arg509 were identified as critical constituents of the XBB.1 variant. Notably, Ala348, Leu441, Tyr451 and Tyr501 manifested with hydrophobic contacts, while His339, Asn343, Ala344, Thr345, Thr346, Lys440, Lys444, Ser446, Asn448, Asn450, Ala484, Arg498, Thr500 and Arg509 exhibited hydrogen bonding. Particularly, Asn448 demonstrated persistent hydrogen bonding throughout the simulation which also corroborating interactional role during molecular docking (Figs. 6 and 7). Furthermore, Asn343, Ala344, Thr345, Asn448, Arg498 and Arg509 were implicated in hydrogen bonding with water bridge formation, which underscores the multifaceted capabilities of ligand anchorage. This suggests that the compound could effectively inhibit the Spike glycoprotein. Furthermore, the presence of all these essential components in *S. Littoreus* enhances their potential therapeutic value in combating life-threatening diseases such as COVID-19.

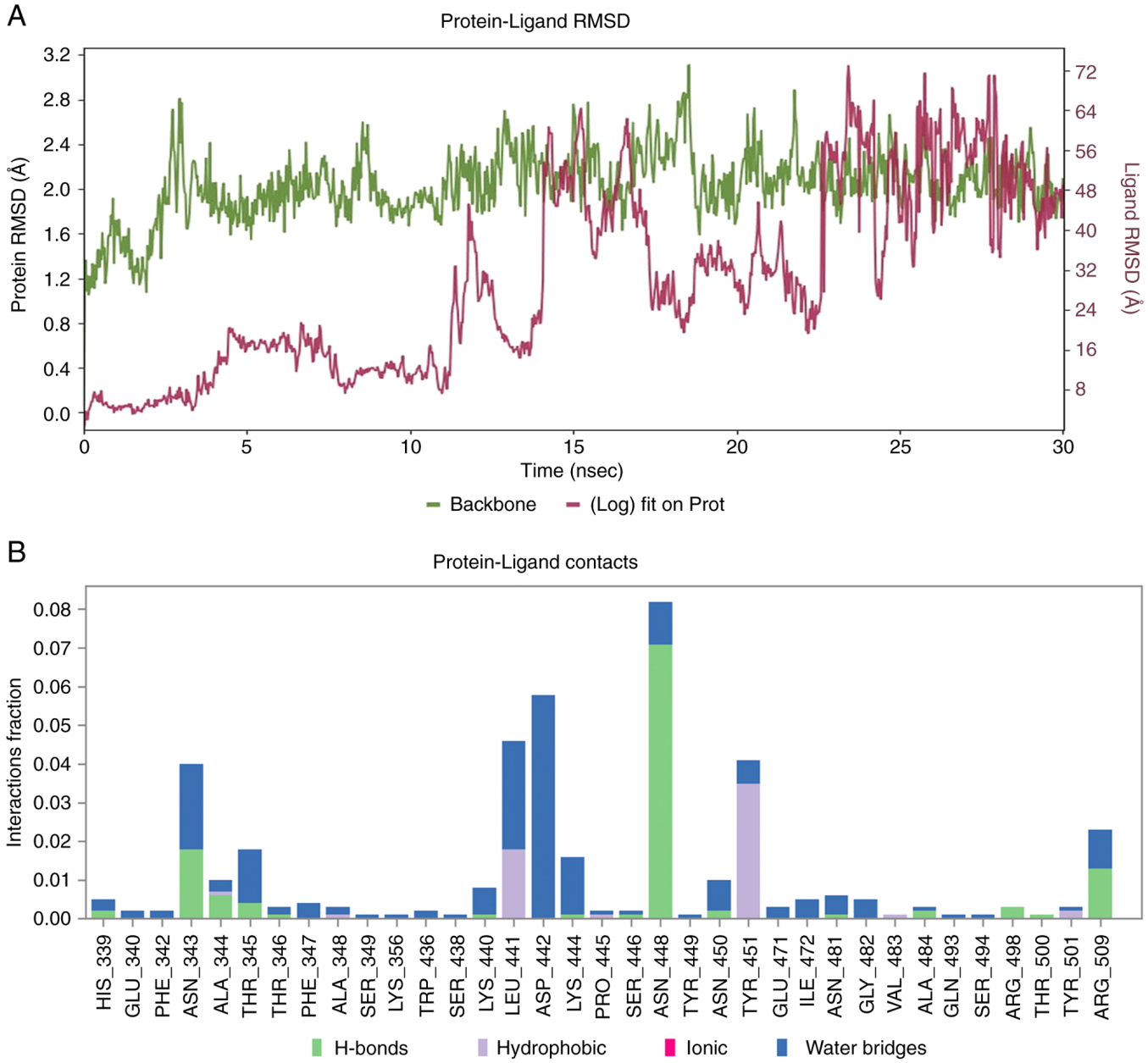

Figure 8. MDS for the SARS-CoV-2 XBB.1 integrated with SL-MHDC. (A) Time-dependent RMSD of the SARS-CoV-2 XBB.1 backbone is shown in green and SL-MHDC ligand is represented in cherry rose with the bounds of 30 nsec trajectory. Equilibrium attains at ~13 nsec within 1.5 Å with negligible non-uniformities. (B) Protein-ligand contacts: Bar chart depicting interaction fractions (x-axis) and interacting residues (y-axis). MDS, molecular dynamics simulations; RMSD, root-mean-square deviation.

In conclusion, in the present study, an innovative *in silico* molecular docking approach was utilized to pinpoint a putative compound for combating severe acute respiratory syndrome caused by coronavirus. The analysis identified the bioactive compound1-methylene-2b-hydroxymethyl-3 ,3-dimethyl-4b-(3-methylbut-2-enyl)-cyclohexane, from the leaf extracts of coastal grass as a potential inhibitor against the SARS-CoV-2 XBB.1 spike glycoprotein (PDB ID: 8IOV). Furthermore, in order to validate the docking results and to shed light on to the stability of protein-ligand interaction, MDS were conducted. Through this process, the binding potential of the complex under dynamic physiological conditions and its structural stability were demonstrated. These findings indicate a possible interaction that necessitates further analysis to determine the therapeutic potential of the compound. Additionally, the present study focused on the test compounds rather than known inhibitors, such as remdesivir and nirmatrelvir; thus, such comparisons need to be included in future studies. Moreover, further investigations of the influence of the compound on the spike-angiotensin-converting enzyme 2 interface could provide a more detailed understanding of its antiviral potential. Nevertheless, further research on its *in vitro* and *in vivo* efficacy against SARS.CoV-2 is imperative for possible clinical translation and patient well-being.

Acknowledgements

The authors are very much grateful to the Rapinat Herbarium and Centre for Molecular Systematics, St. Joseph's College (Autonomous), Tiruchirappalli, Tamil Nadu, India for their support in authenticating the experimental plant.

Funding

No funding was received.

Availability of data and materials

The data generated in the present study may be requested from the corresponding author.

Authors' contributions

JV, INPA and SS conceived and designed the study. JV, INPA, JSM, SKRN, VCS and SS surveyed the scientific literature. JV, INPA, JSM and SS analysed data and wrote the draft manuscript. JV, INPA, SKRN, VCS and SS interpreted the data and reviewed the manuscript. INPA and SS revised the manuscript. All authors have read and approved the final manuscript. INPA and SS confirm the authenticity of all the raw data.

Ethics approval and consent to participate

Not applicable.

Patient consent for publication

Not applicable.

Competing interests

The authors declare that they have no competing interests.

References

1. Morens DM and Fauci AS: Emerging pandemic diseases: How we got to COVID-19. Cell 182: 1077-1092, 2020.
2. Wang W, Xu Y, Gao R, Lu R, Han K, Wu G and Tan W: Detection of SARS-CoV-2 in different types of clinical specimens. JAMA 323: 1843-1844, 2020.
3. Zaki AM, van Boheemen S, Bestebroer TM, Osterhaus AD and Fouchier RA: Isolation of a novel coronavirus from a man with pneumonia in Saudi Arabia. N Engl J Med 367: 1814-1820, 2012.
4. Zhu N, Zhang D, Wang W, Li X, Yang B, Song J, Zhao X, Huang B, Shi W, Lu R, *et al*: A novel coronavirus from patients with Pneumonia in China, 2019. N Engl J Med 382: 727-733, 2020.
5. Pilia E, Belletti A, Fresilli S, Lee TC, Zangrillo A, Finco G and Landoni G; full anticoagulation: The effect of heparin full-dose anticoagulation on survival of hospitalized, non-critically Ill COVID-19 patients: A meta-analysis of high quality studies. Lung 201: 135-147, 2023.
6. Mehta OP, Bhandari P, Raut A, Kacimi SEO and Huy NT: Coronavirus disease (COVID-19): Comprehensive review of clinical presentation. Front Public Health 8: 582932, 2021.
7. Mustafa M, Abbas K, Ahmad R, Ahmad W, Tantry IQ, Islam S, Moinuddin, Alam M, Hassan M, Usmani N and Habib S: Unmasking vulnerabilities in the age of COVID-19 (Review). World Acad Sci J 7: 2, 2025.
8. Cheng F, Li W, Zhou Y, Shen J, Wu Z, Liu G, Lee PW and Tang Y: admet SAR: A comprehensive source and free tool for assessment of chemical ADMET properties. J Chem Inf Model 52: 3099-3105, 2012.
9. Low KO, Md Iqbal N, Ahmad A and Johari N: Detection of SARS-CoV-2 Delta, Omicron and XBB variant using colorimetric reverse-transcription loop-mediated isothermal amplification and specific primers. World Acad Sci J 7: 50, 2025.
10. Hoffmann M, Kleine-Weber H, Schroeder S, Krüger N, Herrler T, Erichsen S, Schiergens TS, Herrler G, Wu NH, Nitsche A, *et al*: SARS-CoV-2 Cell Entry Depends on ACE2 and TMPRSS2 and is blocked by a clinically proven protease inhibitor. Cell 181: 271-280.e8, 2020.
11. Selvavinayagam ST, Karishma SJ, Hemashree K, Yong YK, Suvaithenamudhan S, Rajeshkumar M, Aswathy B, Kalaivani V, Priyanka J, Kumaresan A, *et al*: Clinical characteristics and novel mutations of omicron subvariant XBB in Tamil Nadu, India - a cohort study. Lancet Reg Health Southeast Asia 19: 100272, 2023.
12. Malik YS, Sircar S, Bhat S, Sharun K, Dhama K, Dadar M, Tiwari R and Chaicumpa W: Emerging novel coronavirus (2019-nCoV)-current scenario, evolutionary perspective based on genome analysis and recent developments. Vet Q 40: 68-76, 2020.
13. Zumla A, Chan JF, Azhar EI, Hui DS and Yuen KY: Coronaviruses-drug discovery and therapeutic options. Nat Rev Drug Discov 15: 327-347, 2016.
14. De Wit E, van Doremalen N, Falzarano D and Munster VJ: SARS and MERS: Recent insights into emerging coronaviruses. Nat Rev Microbiol 14: 523-534, 2016.
15. Anand K, Ziebuhr J, Wadhwani P, Mesters JR and Hilgenfeld R: Coronavirus main proteinase (3CLpro) structure: Basis for design of anti-SARS drugs. Science 300: 1763-1767, 2003.
16. Needle D, Lountos GT and Waugh DS: Structures of the Middle East respiratory syndrome coronavirus 3C-like protease reveal insights into substrate specificity. Acta Crystallogr D Biol Crystallogr 71: 1102-1111, 2015.
17. Xu J, Zhao S, Teng T, Abdalla AE, Zhu W, Xie L, Wang Y and Guo X: Systematic comparison of two animal-to-human transmitted human coronaviruses: SARS-CoV-2 and SARS-CoV. Viruses 12: 244, 2020.
18. Talluri S: Computational protein design of bacteriocins based on structural scaffold of aureocin A53. Int J. Bioinformatics Research and Applications 15: 129-143, 2019.
19. Talluri S: Molecular docking and virtual screening based prediction of drugs for COVID-19. Comb Chem High Throughput Screen 24: 716-728, 2021.
20. Jalota K, Sharma V, Agarwal C and Jindal S: Eco-friendly approaches to phytochemical production: Elicitation and beyond. Nat Prod Bioprospect 14: 5, 2024.
21. Wang YM, Ran XK, Riaz M, Yu M, Cai Q, Dou DQ, Metwaly AM, Kang TG and Cai DC: Chemical constituents of stems and leaves of Tagetespatula L. and its fingerprint. Molecules 24: 3911, 2019.
22. Altemimi A, Lakhssassi N, Baharlouei A, Watson DG and Lightfoot DA: Phytochemicals: Extraction, isolation, and identification of bioactive compounds from plant extracts. Plants (Basel) 6: 42, 2017.
23. Vedhamani J, Ajithkumar IP and Jemima EA: Exploring the in vitro antimicrobial, antioxidant, and anticancer potentials of Spinifex littoreus Burm f. Merr. against human cervical cancer. Plant Sci Today 11: 242-251, 2024.
24. Connor HE: Breeding systems in Indomalesian Spinifex (Paniceae: Gramineae). BLUMEA 41: 445-454, 1996.
25. Sen UK and Bhakat RK: Ethnobotanical study on sand-dune based medicinal plants and traditional therapies in coastal Purba Medinipur District, West Bengal, India. Eur J Med Plants 26: 1-19, 2019.
26. Neamsuvan O, Singdam P, Yingcharoen K and Sengnon N: A survey of medicinal plants in mangrove and beach forests from sating Phra Peninsula, Songkhla Province, Thailand. J Med Plants Res 6: 2421-2437, 2012.
27. Shakila K: Bioactive Flavonids of Spinifex littoreus (Burm. f.) merr-investigation by elisa method. J Stress Physiol Biochem 16: 107-112, 2020.
28. Thirunavukkarasu P, Ramanathan T, Ramkumar L and Balasubramanian T: Anti microbial effect of a coastal sand dune plant of Spinifex littoreus (Burm. f.) Merr. Curr Res J Biol Sci 2: 283-285, 2010.
29. Dampalla CS, Kim Y, Bickmeier N, Rathnayake AD, Nguyen HN, Zheng J, Kashipathy MM, Baird MA, Battaile KP, Lovell S, *et al*: Structure-guided design of conformationally constrained cyclohexane inhibitors of severe acute respiratory syndrome coronavirus-2 3CL protease. J Med Chem 64: 10047-10058, 2021.

30. Nallaiyah VJ and Newton PAI: Antimicrobial and larvicidal efficacy of the methanolic extract of Spinifex littoreus (Burm F.) Merr. Biotech Res Asia 21, 1575-1582, 2024.
31. Redfern J, Kinninmonth M, Burdass D and Verran J: Using soxhlet ethanol extraction to produce and test plant material (essential oils) for their antimicrobial properties. J Microbiol Biol Educ 15: 45-46, 2014.
32. Geetha TS and Geetha N: Phytochemical screening, quantitative analysis of primary and secondary metabolites of Cymbopogancitratus (DC) Stapf. leaves from Kodaikanal hills, Tamilnadu. Int J Pharm Tech Res 6: 521-529, 2014.
33. Arya V, Thakur N and Kashyap CP: Preliminary phytochemical analysis of the extracts of Psidium leaves. Journal of Pharmacognosy and Phytochemistry 1: 1-5, 2012.
34. Mohammed J, Oba OA and Aydinlik NP: Preliminary phytochemical screening, gc-ms, FT-IR analysis of ethanolic extracts of Rosmarinus Officinalis, Coriandrum Sativum L. and Mentha Spicata. Hacettepe J Biol Chem 51: 93-102, 2023.
35. Jose JK, Sudhakaran S, Sony J and Variyar E: A comparative evaluation of anticancer activities of flavonoids isolated from Mimosa pudica, Aloe vera and Phyllanthus niruri against human breast carcinoma cell line (MCF-7) using MTT assay. Int J Pharm Pharmaceut Sci 6: 319-322, 2014.
36. Ayoola GA, Coker HAB, Adesegun SA, Adepoju-Bello AA, Obaweya K, Ezennia EC and Atangbayila TO: Phytochemical screening and antioxidant activities of some selected -3medicinal plants used for malaria therapy in Southwestern Nigeria. Trop J Pharm Res 7: 1019-1024, 2008.
37. Yusuf AZ, Zakir A, Shemau Z, Abdullahi M and Halima SA: Phytochemical analysis of the methanol leaves extract of Paullinia pinnata linn. J. Pharmacognosy Phytother6: 10-16, 2014.
38. Krishnaiah D, Sarbatly R and Bono A: Phytochemical antioxidants for health and medicine: A move towards nature. Biotechnol Mol Biol Rev 1: 097-104, 2007.
39. Sandosh TA, Peter MPJ and Raj JY: Phytochemical analysis of Stylosanthesfruticosa using UV-VIS, FTIR and GC-MS. Res J Chem Sci 3: 14-23, 2013.
40. Shamsa F, Monsef H, Ghamooshi R and Verdian-Rizi M: Spectrophotometric determination of total alkaloids in some Iranian medicinal plants. Thai J Pharm Sci 32: 17-20, 2008.
41. Ghorai N, Chakraborty S, Gucchait S, Saha SK and Biswas S: Estimation of total Terpenoids concentration in plant tissues using a monoterpene, Linalool as standard reagent. Protocol Exchange: 1-6: 2012.
42. Marinova D, Ribarova F and Atanassova M: Total phenolics and flavonoids in Bulgarian fruits and vegetables. JU Chem Metal 40: 255-260, 2005.
43. Van Buren JP and Robinson WB: Formation of complexes between protein and tannic acid. J Agric Food Chem 17: 772-777, 1969.
44. Taylor B: The International System of Units (SI), 2008 Edition, Special Publication (NIST SP). National Institute of Standards and Technology, Gaithersburg, MD, 2008. Accessed on July 8, 2025. https://doi.org/10.6028/NIST.SP.330e2008
45. Iordache A, Culea M, Gherman C and Cozar O: Characterization of some plant extracts by GC-MS. Nucl Instrum Methods Phys Res B 267: 338-342, 2009.
46. Daina A, Michielin O and Zoete V: SwissADME: A free web tool to evaluate pharmacokinetics, drug-likeness and medicinal chemistry friendliness of small molecules. Sci Rep 7: 42717, 2017.
47. Eberhardt J, Santos-Martins D, Tillack AF and Forli S: AutoDock Vina 1.2.0: New docking methods, expanded force field, and python bindings. J Chem Inf Model 61: 3891-3898, 2021.
48. Trott O and Olson AJ: AutoDock Vina: Improving the speed and accuracy of docking with a new scoring function, efficient optimization, and multithreading. J Comput Chem 31:455-461, 2010.
49. Morris GM, Huey R, Lindstrom W, Sanner MF, Belew RK, Goodsell DS and Olson AJ: AutoDock4 and AutoDockTools4: Automated docking with selective receptor flexibility. J Comput Chem 30: 2785-2791, 2009.
50. Bowers KJ, Chow E, Xu H, Dror RO, Eastwood MP, Gregersen BA, Klepeis JL, Kolossvary I, Moraes MA, Sacerdoti FD, *et al*: Scalable algorithms for molecular dynamics simulations on commodity clusters'. Proceedings of the ACM/IEEE SC2006 Conference on High Performance Networking and Computing, New York, NY, 11-17, 2006.
51. Ajuru MG, Williams LF and Ajuru G: Qualitative and quantitative phytochemical screening of some plants used in ethnomedicine in the Niger Delta region of Nigeria. J Food Nutr Sci 5: 198-205, 2017.
52. Rechab SO, Ngugi CM, Maina EG, Madivoli ES, Kareru PG, Mutembei JK, Kairigo PK, Cheruiyot K and Ruto MC: Antioxidant activity and antimicrobial properties of *Entadaleptostachya* and *Prosopisjuliflora* extracts. J Med Plants Econ Dev 2: 1-8, 2018.
53. Chandran M, Vivek P and Kesavan D: Phytochemical screening and anti-bacterial studies in salt marsh plant extracts (*Spinifex Littoreus* (Burm. f) Merr. and *Heliotropium Curassavicum* L.). Recent Trends Biotechnol Chem Eng 6: 4307-11, 2014.
54. Koche D, Shirsat R and Kawale MA: An overview of major classes of phytochemicals: their types and role in disease prevention. Hislopia J 9: 1-11, 2016.
55. Shirsat R, Suradkar S and Koche D: Some phenolic compounds from *Salvia plebeia*. Biosci Discov 3: 61-63, 2012.
56. Wink M, Schmeller T and Latz-Brüning B: Modes of action of allelochemical alkaloids: Interaction with neuroreceptors, DNA, and other molecular targets. J Chem Ecol 24: 1881-1937, 1998.
57. Langenheim JH: Higher plant terpenoids: A phytocentric overview of their ecological roles. J Chem Ecol 20: 1223-1280, 1994.
58. Dudareva N, Pichersky E and Gershenzon J: Biochemistry of plant volatiles. Plant Physiol 135: 1893-1902, 2004.
59. Dai J and Mumper RJ: Plant phenolics: Extraction, analysis and their antioxidant and anticancer properties. Molecules 15: 7313-7352, 2010.
60. Khatri S, Paramanya A and Ali A: Phenolic acids and their health-promoting activity. Plant Human Health 2: 661-680, 2019.
61. Singh B and Sharma RA: Plant terpenes: defense responses, phylogenetic analysis, regulation and clinical applications. 3 Biotech 5: 129-151, 2015.
62. Thoppil RJ and Bishayee A: Terpenoids as potential chemopreventive and therapeutic agents in liver cancer. World J Hepatol 3: 228-249, 2011.
63. Subiono T, Sadarudin and Tavip MA: Qualitative and quantitative phytochemicals of leaves, bark and roots of *Antiaris toxicaria* Lesch, a promising natural medicinal plant and source of pesticides. Plant Sci Today 10: 5-10, 2023.
64. Ouandaogo HS, Diallo S, Odari E and Kinyua J: Phytochemical Screening and GC-MS Analysis of Methanolic and Aqueous Extracts of Ocimum kilimandscharicum Leaves. ACS Omega 8: 47560-47572, 2023.
65. Konappa N, Udayashankar AC, Krishnamurthy S, Pradeep CK, Chowdappa S and Jogaiah S: GC-MS analysis of phytoconstituents from Amomum nilgiricum and molecular docking interactions of bioactive serverogenin acetate with target proteins. Sci Rep 10: 16438, 2020.
66. Iikasha AMN, Bock R and Mumbengegwi DR: Phytochemical screening and antibacterial activity of selected medicinal plants against laboratory diarrheal bacteria strains. J Pharmacogn Phytochem 6: 2337-2342, 2017.
67. Tiwari P, Kumar B, Kaur M, Kaur G and Kaur H: Phytochemical screening and extraction: A review. Int Pharm Sci 1: 98-106, 2011.
68. Ponnamma SU and Manjunath K: GC-MS Analysis of phytocomponents in the methanolic extract of *Justiciawynaadensis* (nees) T. anders. Int J Pharm Bio Sci 3: 570-576, 2012.
69. Kim DH, Park MH, Choi YJ, Chung KW, Park CH, Jang EJ, An HJ, Yu BP and Chung HY: Molecular study of dietary heptadecane for the anti-inflammatory modulation of NF-kB in the aged kidney. PLoS One 8: e59316, 2013.
70. Marrufo T, Nazzaro F, Mancini E, Fratianni F, Coppola R, De Martino L, Agostinho AB and De Feo V: Chemical composition and biological activity of the essential oil from leaves of Moringa oleifera Lam. cultivated in Mozambique. Molecules 18: 10989-11000, 2013.
71. Ma J, Xu RR, Lu Y, Ren DF and Lu J: Composition, antiproliferative, and antioxidant activity of cold-pressed seed oils from Paeonialactiflora and Paeoniaostii. J Food Sci 80: 2465-2474, 2015.
72. Katz DH, Marcelletti JF, Khalil MH, Pope LE and Katz LR: Antiviral activity of 1-docosanol, an inhibitor of lipid-enveloped viruses including herpes simplex. Proc Natl Acad Sci 88: 10825-10829, 1991.